

BR8715444



K-SHELL IONIZATION CROSS SECTIONS FOR
W, Au AND U BY LOW VELOCITY PROTONS*

R.V. de Castro Faria, F.L. Fraire Jr., E. C. Montenegro, A.
C. de Pinho and J. P. de Silveira**

Departamento de Física, Pontifícia Universidade Católica
Rio de Janeiro, Brasil***

ABSTRACT - Proton-induced K-shell ionization cross section for W, Au and U by low velocity protons were obtained from thick target measurements. For the first time the lowest incident energy reached a value less than 10 times the binding energy of the K-shell electron (less than 9 times in the case of Au). Possible errors are thoroughly examined and a comparison with other available experimental results and theoretical values is presented and discussed.

RESUMO - Foram obtidas seções de choque de ionização da camada K do W, Au e U por prótons com energias entre 0.65 e 3.74 MeV. Os resultados experimentais são comparados com valores teóricos calculados na aproximação de Born de onda plana e as aproximações semi-clássica. Em particular, são discutidas as correções da trajetória, energia de ligação e relativística, assim como, o aspecto inelástico de colisões a baixas velocidades.

* To be published in the Journal of Physics B: At.Mol.Phys.

** Supported by Financiadora de Estudos e Projetos (FINEP).

*** Postal address: PUC-RJ, CP 36771, RJ 22453, Brasil

1. INTRODUCTION

Although during the recent years an important number of measurements of cross sections for K-shell ionisation by swift bare light nuclei have been performed with increasing accuracy and although many refined calculations, including sophisticated corrections, have been performed, significant discrepancies persist when experimental and theoretical results are put together. In part these discrepancies come from the difficulty in determining absolute cross sections. Experimental data are quoted with typically individual uncertainties of 5 to 15%. However, when measurements of different groups are compared, discrepancies of about five or more standard deviations are not unusual. Systematic errors come mainly from the determination of the overall detection efficiency and from the reduction of the rough experimental data and can not be treated as statistical fluctuations. On the other hand, it is unquestionable that some ambiguities remain in the way the multiple corrections are handled when introduced into the basic models (PWBA or SCA) that describe the direct Coulomb excitation of an electron from the K-shell into the continuum by a point-like charged particle.

This situation has been periodically reviewed in a series of workshops on inner shell ionisation by heavy

particles (see for example Paul 1980 and 1982, Kocbach et al 1979, Lamb et al 1982 and references therein, see also Rice 1981 and Paul and Oberman 1983).

Differences between experimental and theoretical results are more evident in the low impact velocity region. In these conditions the problems are twofold. Besides the currently admitted effects of the increased binding, the relativistic modifications of the electronic wave functions and the deflection of the projectile trajectory by the electric field of the target nucleus which become much more sensitive to details in their calculations and mutual dependence, other corrections become important. On the other hand, the cross sections become so small that the use of thick targets and high currents is imperative. The X-ray yields become hard to be accurately measured since the subtraction of the background is no longer a trivial problem and the effects of the energy loss of the incident particles inside the target become increasingly important. To extract X-ray production cross sections from the rough data is inherently less precise than in the thin-target transmission technique.

In this paper we present some accurate measurements on the K-shell ionization cross sections of W, Au and U by protons in the lowest energy region thus far reported.

Typical uncertainties of cross-section measurements are 10-15%. At these energies the usual assumption that the binding energy of the shell can be neglected with respect to the total energy in the center of mass system can no longer be sustained. The inelasticity of the ionization process, as well the three above mentioned corrections are incorporated to the FWER calculations for the sake of comparison between experimental and calculated results.

2. EXPERIMENTAL PROCEDURE

The experimental setup for the present measurements has already been given in detail elsewhere (Barros Leite et al. 1977, Justimiano et al. 1980, de Castro Faria et al. 1983). Only the description relevant to the present experiment is given here. Momentum analysed incident beams of protons were obtained from the EMBE 4.07 Van de Graaff Accelerator at the Catholic University of Rio de Janeiro. The analysed beam was focused by quadrupole lenses, deflected 30° by a switching magnet and then collimated by two tantalum apertures with 2mm and 3mm diameters and 30cm apart. The last collimator was located 5cm before the entrance of the insulated target chamber and 27cm upstream from the target holder.

The energy resolution of the accelerator and bending

magnet was monitored by the well-known and very strong resonances observed in the $^{27}\text{Al}(p, \alpha)^{24}\text{Mg}$ reaction. The resonance at 1184 keV gave the absolute calibration and the others resonances in this region of energy were used to check the linearity of the accelerator-energy setting. The width (FWHM) of the 1184 keV resonance was observed to be equal to 1.8 keV. The stability during each run was best than this width.

The total running time was of about 10^3 hours and some individual runs were as long as 87 hours. Depending on the count rate, currents from 30 up to 500 nA were used. Dead time corrections were kept negligible as compared to statistical fluctuations in the number of counts at the K_{α} peaks.

Since the L and M x-ray production cross sections are many orders of magnitude larger than the K-x-ray cross section a 0.1mm Ge foil was positioned in front of the x-ray detector. This detector, placed at 90° to the beam, was a high-purity Ge detector with a measured resolution (FWHM) of 340 eV at 59.5 keV. The overall absolute efficiency of the x-ray detector was determined in the standard manner using calibrated radioactive sources of ^{57}Co , ^{109}Cd and ^{241}Am located at the target position. Uncertainties of no more than 5% are expected for the absolute efficiencies.

Thick targets were employed. The gold target was a 1.75 mg/cm^2 foil and the tungsten and uranium targets were thick enough to stop the most energetic bombarding protons.

Special care was taken with the shielding of the detection system. Even without an incident beam an appreciable background was observed coming from the environment (mainly Compton photons from the ^{40}K decay and from decays in the natural radioactive series). Moreover, an energy dependent background, which originated at the magnets, slits and collimators, appears with the beam on. The detector was surrounded by 10cm thick lead blocks and 1.2 cm iron plates which reduced by a factor of 10 the background in the region of the gamma-ray spectra from -50 to -120 keV. It was observed that the uranium target itself was the source of an important background, viz. U x-rays induced by the emitted alpha particles. The subtraction of this background in the spectra obtained at very low incident energies is the main source of statistical errors in the U x-ray production cross section.

Normalization of the measurements was made by measuring the charge collected by the entire target chamber. The insulation was better than $10^{13}\Omega$. In the case of the gold target a Si surface barrier detector was mounted at 90° to the incident beam direction, facing the x-ray detector, to detect the Rutherford elastically scattered protons transmitted

through the target. It was equipped with a 0.5mm collimator to prevent high count rates at low incident energies.

With all the targets, Coulomb excited nuclear gamma rays were observed. They became relatively more important with respect to the K x-rays as the incident energy decreased. They presented no special problem in all cases except with the W target. Internal conversion of the transition from the first excited state to the ground state in ^{182}W , ^{183}W , ^{184}W and ^{186}W contributed to about 5% of the K x-rays at 3.75 MeV incident protons and 20% at 0.65 MeV. Theoretical α_2 internal conversion coefficients (Sliv and Band 1956) were used to estimate this contribution.

The $K_{\alpha_1}/K_{\alpha_2}$ ratio was verified to be independent from the incident energy. An average ratio was determined from the best statistics spectra and this ratio was employed as a test to verify if the background was correctly subtracted in the poorer statistics spectra.

In almost all the cases the K_{β_1}/K_{α_2} branching ratio could be precisely measured. For the gold target a Coulomb excited nuclear transition overlaps the K_{β_1} peak and became important below proton energies of about 1.25 MeV. The K_{β_1}/K_{α_2} ratios were in good agreement with the values reported by Salem et al. (1974). No indication of simultaneous ionizations of K, L, M and N shells was observed in any of the proton

energies. Effects larger than 1% are not expected from the theory.

The background under the peaks was always flat and easy to be taken off. Care must be exercised in obtaining the areas of the K_{α_1} peak since the low energy tail of the K_{α_1} photopeak present under the K_{α_2} photopeak must be subtracted. In order to obtain the x-ray yields produced by the proton ionization of the target atoms, the areas under the K_{α_1} and K_{α_2} peaks were corrected for efficiency detection, summed over and multiplied by the following ($K_{\alpha_1} + K_{\alpha_2}$)/ K_{α} ratios: 1.275 for W, 1.27% for Au and 1.26% for U. Errors in the K_{β}/K_{α} ratios are supposed to be less than 1%.

Statistical errors in the K_{α} yields ranged from less than 1% in the best statistics spectra up to 5% in the case where K_{α} x-rays from background (U) or internal conversion (W) became important. The fluorescence yields have been taken from the compilation of Bambynek et al (1972). There is no significant difference between these values and the most recent ones (Krause 1979) for the elements of this work.

Figure 1 shows two spectra of the tungsten K x-rays. The lower spectrum was obtained at the lowest incident energy (650 keV proton beam) and the other, with a much better statistics, corresponds to 2.75 MeV incident energy.

3. DATA ANALYSIS AND RESULTS

When thick targets are employed the number of observed x-rays is given by

$$N_x = \frac{Q\epsilon}{4\pi} \cdot Pn \int_0^{t/\cos\theta} e^{-\mu x} \cos\theta/\cos\phi Q(x) dx \quad (1)$$

where $Q\epsilon$ is the product of the acceptance solid angle and the efficiency of detection, n is the atomic density in the target and P is number of incident protons. The angles θ and ϕ are formed, respectively, by the beam direction and by the line of sight from the beam spot to the detector with respect to the normal of the target surface at the point of beam impact. The impact direction defines the x -axis and t is the thickness of the target. In the present experiment $\theta = \phi = 45^\circ$. Here $Q(x)$ is the x-ray production cross section at the point of coordinate x where the energy is no more the incident energy E_1 but

$$E(x) = E_1 - \int_0^x S(E) dx \quad (2)$$

where $S(E) = |dE/ds|$ is the absolute value of target stopping power for projectiles of energy $E(x)$. The absorption coefficient of the target for its own x rays is μ .

Defining $Y_x(E_1)$ as the x-ray yield registered by the detector per incident proton and $\gamma = Q\epsilon/4\pi$ as the overall detection efficiency, it follows (Gray 1980) that the x-ray production cross section when all the incident particles are stopped in the target ($t = \infty$) can be written as

$$\sigma_x(E_1) = \frac{1}{dY} \left[S(E_1) \frac{dY(E)}{dE} \left\{ E - E_1 + v Y_x(E_1) \right\} \right] \quad (3)$$

Once $Y_x(E_1)$ is measured, and since $S(E)$ and v are well known quantities, the problem is the precise calculation of the slope of Y_x with regard to E_1 . Our yield curves were fitted with the following type of function

$$Y_x(E) = aE^2(1+bE^2)\exp(-cE^{-3/2}) \quad (4)$$

Figure 2 shows the quality of the fit for the three different targets and gives the four adjustable parameters a , b , c and δ . The root-mean-square deviations of the fitted yields from the experimental values are 1% for Au, 2% for W and 5% for U. The contribution of the second term of equation (3) is always less than 1% of that of the first term. Of course this fitting procedure is an important source of error but it is very comfortable to represent $Y_x(E)$ by a function which can be differentiated analytically.

The stopping powers employed in the calculation of σ_x were taken from the analytical fittings of Andersen and Siegler (1977) and Montenegro et al. (1982). The two sets differ by less than 1% in the region of interest. The absorption coefficients were those of Vingale (1973).

The thickness of the gold target could not be considered infinite but it was not thin enough so that the

usual simple corrections could be applied. Rutherford scattering was used for absolute normalization purposes. Calling E_2 the energy of the proton after traversing the target we can write, neglecting from the beginning the self absorption of the α -rays,

$$N_N = \frac{Q_d}{4\pi} P_N \int_{E_2}^{E_1} \frac{\sigma_N(E)}{S(E)} dE \quad (5a)$$

and

$$N_p = \frac{Q_d \epsilon_p}{P_p} P_N \int_{E_2}^{E_1} \frac{(d\sigma_N(E)/d\Omega)}{S(E)} dE \quad (5b)$$

where $Q_d \epsilon_p$ is the overall detection efficiency for the scattered protons (in our energy range $\epsilon_p = 1$), N_p is the number of observed protons and $d\sigma_N/d\Omega$ is the differential Rutherford scattering cross section.

From equation (5a) it follows that

$$\begin{aligned} \frac{1}{P_N} \frac{dN_N}{dE_1} &= \frac{\sigma_N(E_1)}{S(E_1)} - \frac{\sigma_N(E_2)}{S(E_2)} \frac{dE_2}{dE_1} \\ &= [\sigma_N(E_1) - \sigma_N(E_2)]/S(E_1) \end{aligned} \quad (6)$$

Then

$$\sigma_N(E_1) - \sigma_N(E_2) = \frac{1}{P_N} \frac{dN_N(E_1, t)}{dE_1} S(E_1) = g(E_1, t)/P_N \quad (7)$$

Of course for a target where the incident proton loses all its energy

$$j_x(E_1) = g(E_1)/\gamma n$$

In agreement with equation (1) if the self-absorption of the x-rays is not considered.

Since the function g can be constructed point by point from the fitted yield curve and the stopping power curve, it is possible to calculate

$$j_x(E_1) - \sigma_x(E_m) = (1/\gamma n) \sum_{i=1}^m g_i \quad (8)$$

where $g_1 = g(E_1)$, $g_2 = g(E_2)$ and so forth.

As $E_m \ll E_1$ we have $n_x(E_m) \ll \sigma_x(E_1)$ and the summation can be truncated after a relatively small number of steps. Then

$$\sigma_x(E) = (1/\gamma n) \sum_{i=1}^m g_i \quad (9)$$

On the other hand

$$Y_p = n_p/P = \sigma_p n \left. \frac{d\sigma_p}{dE} \right|_{E_1, E_2} \int_{E_2}^{E_1} \frac{dE}{E^2 S(E)} \quad (10)$$

The simultaneous determinations of Y_x and Y_p allows us to write

$$\sigma_x(E_1) = (\sigma_p/\gamma) (Y_p(E_1)/E_1^2)^{-1} \left. \frac{d\sigma_p}{dE} \right|_{E_1} \left(\sum_{i=1}^m g_i \right) \int_{E_2}^{E_1} \frac{dE}{E^2 S(E)} \quad (11)$$

From the definition

$$t/\cos\theta = \int_{E_2}^{E_1} dE/\beta(E) . \quad (12)$$

E_2 is easily obtained in terms of E_1 and t , since a linear approximation for $\beta^{-1}(E)$ is quite satisfactory. The integral appearing in equation (12) can be evaluated within the same approximation.

The resulting K-shell ionisation cross sections are presented in table I and in figure 3 where measured values from other works are also shown (Anholt 1978a, Kamiya et al. 1977, Goclowski et al. 1983). Whenever there are other published results the agreement is usually within experimental uncertainties.

Sources of experimental uncertainties are tabulated in table II. The uncertainties in the ratios of nearby cross sections are typically 2/3 of those of the absolute cross sections.

4. DISCUSSION AND CONCLUSIONS

The solid curve presented in figure 3 are standard MNSA calculations (Rice et al. 1977) with the following corrections: 1) the effects of increased binding of the K-shell electron are introduced through reduced variables in the MNSA according to the PSS theory (Brandt et al.1966,

Bashas et al. 1973, Bashas et al. 1978), ii) the relativistic effects which become important for high- Z_2 targets are incorporated following the prescriptions of Brandt and Lapicki (1979), iii) the effects of the deflection and deceleration of bombarding particle in the field of the target nucleus is described by the analytical expression derived by Montenegro and de Fiufo (1982) which reproduces the numerical calculations of Kocbach (1976) for protons incident on gold. This triple choice deserves some comments. The adopted binding correction is by far the most popular one. It is calculated following a perturbative procedure with hydrogenic non-relativistic wavefunctions. The relativistic correction seems in reasonable agreement with recent calculations (Mukoyama and Sarkadi 1983) using hydrogenic Dirac wavefunctions. Other available relativistic corrections presented as multiplicative factors (Anholt 1978b and references therein) give results that agree within 20% with the results of Brandt and Lapicki in the energy range considered in this work. Much larger differences can be observed between the adopted Coulomb factor and others that can be found in the literature. These differences can be as large as an order of magnitude in very adiabatic collisions (see Paul 1982 and Kocbach et al. 1980). Also important is the order in which these corrections are in-

roduced. Firstly the binding energy was corrected. Then relativistic and Coulomb deflection effects were calculated with the modified binding energy but the effective velocity resulting from the relativistic correction does not appear in the Coulomb factor.

However, many important aspects of the ionisation by low-velocity ions were not considered. For instance, dipole and recoil effects were ignored. The importance of the dipole amplitude including recoil for low projectile energies was discussed by many authors (Kochbach et al. 1980, Gunderson et al. 1982 and Kiseel et al. 1982). It was shown that in some cases a strong cancellation effect of the dipole term due to the recoil can occur. Moreover, since the effect is more pronounced for small projectile impact parameters it is not expected that the total cross sections would be significantly modified.

The wavefunctions of the electron in the initial and final states employed in the standard PWBA calculations are hydrogenic non relativistic or relativistic wavefunctions. The use of more realistic relativistic Hartree-Fock-Slater wavefunctions could improve the results but does not seem responsible for major modifications with respect to relativistic hydrogenic wavefunctions with an effective charge

for heavy atoms (Trautman and Rösel 1980).

In addition, there are effects concerning the energy loss of slow projectiles during the inelastic ionisation process. On the one hand, the limits of integration usually adopted in the PWBA calculations are not the exact physical limits of integration given by the energy and momentum conservation laws. Benka and Xropf (1978) pointed out the importance of considering the exact limits at low projectile energies. The simulation of this effect through multiplicative correction factors or through effective values of the variables was discussed by Brandt and Lapicki (1981) and by Montenegro et al. (1981), respectively. On the other hand, the Coulomb-deflection factor involves the variables d , which is the half-distance of closest approach in a head-on collision, and q_0 , the minimum momentum transfer for ionisation in units of \hbar . As pointed out by Bang and Manstean (1959) both variables must be suitably modified to take into account the energy loss of the projectile. These authors proposed the same prescription usually applied to nuclear Coulomb excitation, namely, the symmetrisation of the variables.

Even the strict applicability of the PWBA or SCA descriptions in the region of extreme adiabaticity could be

a matter of discussion.

Then the very impressive agreement between experimental and the PWB&RC curves presented in Figure 3 may be partially fortuitous.

In this work the main effort was to measure ionization cross sections for heavy atoms at incident energies where the electron binding energy represents as much as 10% of E_1 . Of course, it is no longer reasonable to disregard, among other effects, the so-called energy-loss effects. These effects become more transparent when we compare figures 4 and 5. In figure 4 our experimental points are plotted against the conventional argument $\sigma_{dq,\zeta}$. The abscissa is the experimental cross sections divided by the calculated PWB&RC (or PSSR) cross sections as described before. Here ζ is the binding correction factor (Babas et al. 1978). The ratio $\sigma_{exp}/\sigma_{PSSR}$ gives the empirical Coulomb-deflection factor which is compared with the correction factors proposed by Babas et al (1978) and by Montenegro and de Pinho (1981). Also shown are the results of the numerical integration of Kocbach (1976) for protons on gold. The approximation suggested by Anholt (1978b) is not shown since it was constructed to fit the numerical factor of Kocbach. As expected from figure 3, the agreement with the Kocbach's and Montenegro and the Pinho's calculations for protons on gold is quite satisfactory.

In figure 5 the exact limits of integration were taken into account in the calculation of the cross sections and the factor dq was modified following the recipe of Brandt and Lapicki (1981) in order to take into account the projectile energy loss in the inelastic collision. The consideration of the inelastic aspect of the collisions introduces a considerable dispersion among the points. Obviously something more is indispensable to recover the previous good agreement. The internal consistency of all published experimental data, even with measurements performed and analyzed in very different ways, points to the need of a more complete and consistent theoretical description of the whole situation.

REFERENCES

- Arundsen P A 1977 J.Phys. B: At. Mol. Phys. 10 2177.
 Anderson B H and Siegler J F 1977 Hydrogen stopping powers and ranges in all elements, Pergamon, New York.
 Anholt R 1978a Phys. Rev. A 17 974.
 Anholt R 1978b Phys. Rev. A 17 983.
 Bambynek M, Gresemann B, Fink R M, Freund H U, Mark A, Swift C D, Price R E and Venugopala Rao P 1972 Rev. Mod. Phys. 44 716.

- Bang J and Hansteen J M 1959 Mat. Fys. Medd. Dan. Vid. Selsk. 31 no. 13.
- Barron Leite C V, de Castro Faria M V, and de Pinho A G 1977 Phys.Rev. A 15 943
- Basbas G, Brandt W, and Laubert R 1973 Phys. Rev. A 7 983.
- Basbas G, Brandt W, and Laubert R 1978 Phys. Rev. A 17 1655.
- Banks O and Kropf A 1978 At. Data Nucl. Data Tables 22 219.
- Brandt W, Laubert R and Selling I 1966 Phys.Lett. 21 518.
- Brandt W and Lapicki G 1979 Phys. Rev. A 20 465
- Brandt W and Lapicki G 1981 Phys. Rev. A 23 1717.
- de Castro Faria M V, Freire Jr F L, de Pinho A G and da Silveira R F 1983 Phys. Rev. A 28 2270.
- Gociowski M, Jankola M, Szarypo J, Hornshoj P and Zalazny S 1983 J.Phys.B: At. Mol. Phys. 16 3571
- Gray T J 1980 in Methods of Experimental Physics 17 ed. P Richard (New York: Academic).
- Quodergsen R, Hansteen J M and Kochbach L 1982 Nucl. Inst.Meth. 192 63.
- Justiniano E L B, Nader A A G, de Castro Faria M V, Barron Leite C V and de Pinho A.G. 1980 Phys. Rev. A 21 73.
- Kamiya M, Ishii K, Sera K, Morita S and Tawara H 1977 Phys. Rev. A 16 2295.
- Kochbach L 1976 Phys. Norv. 8 107.

- Reobach L, Hansteen J M and Gundersen R 1980 Nucl.Inst.Meth.
169 281.
- Krause M O 1979 J.Phys. Chem. Ref. Data 8 307.
- Land D J, Brown M D, Simons D G and Brennan G 1982 Nucl.Inst.
Meth. 192 53.
- Montenegro R C, de Pinho A G and Barros Leite C V 1981 J.Phys.
B: At.Mol. Phys. 14 1991.
- Montenegro R C and de Pinho A G 1982 J.Phys.B: At.Mol.Phys.
15 1521.
- Montenegro R C, Cruz S A and Vargas-Aburto C 1982 Phys. Lett.
92 A 195.
- Mukoyama T and Sarkadi L 1983 Phys. Rev. A 28 1303.
- Paul H 1980 Nucl. Inst. Meth. 169 249.
- Paul H 1982 Nucl. Inst. Meth. 192 41.
- Paul H and Obermann W 1983 Nucl. Inst. Meth. 214 15.
- Rice R, Nesban G and McDaniel F D 1977 At. Data and Nucl.
Data Tables 20 503.
- Rice R R, McDaniel F D, Nesban G and Luggan J L 1981 Phys.
Rev. A 24 750.
- Rösel F, Trautmann D and Baur G 1982 Nucl.Inst.Meth. 192 43.
- Selen S I, Panossian S L and Krause R A 1974 At.Data Nucl.
Data Tables 14 91.
- Sliv L A and Band I M 1956, Coefficients of Internal Conversion

of Gamma Radiation, Academy of Sciences of the USSR,
Moscow-Leningrad, Part I.

Trautmann D and Rösel P 1980 Nucl. Inst. Meth. 169 259.

Veigele W M J 1973 At. Data Tables 5 51.

CAPTIONS TO TABLES

Table I - Measured K-shell ionisation cross section in barns.
Numbers in parentheses indicate powers of 10. See
table II for a discussion on the experimental errors.

Table II - Experimental uncertainties.

TABLE I

W $\mu_K = 0.957$		Au $\mu_K = 0.964$		U $\mu_K = 0.976$	
E_1 (MeV)	σ_K^I (b)	E_1 (MeV)	σ_K^I (b)	E_1 (MeV)	σ_K^I (b)
3.75	7.68(-2)	3.50	2.80(-2)	2.75	3.69(-3)
3.50	5.53(-2)	3.00	1.75(-2)	2.50	2.28(-3)
3.25	4.46(-2)	2.50	9.59(-3)	2.25	1.32(-3)
3.00	3.33(-2)	2.25	6.54(-3)	2.00	6.94(-4)
2.75	2.35(-2)	2.00	4.10(-3)	1.80	3.89(-4)
2.50	1.63(-2)	1.75	2.29(-3)	1.50	1.98(-4)
2.25	1.07(-2)	1.50	1.09(-3)	1.40	8.80(-5)
2.00	6.86(-3)	1.25	4.00(-4)	1.30	5.43(-5)
1.75	3.97(-3)	1.00	9.27(-5)	1.20	3.20(-5)
1.50	2.10(-3)	0.90	4.04(-5)	1.10	1.71(-5)
1.25	9.39(-4)	0.82	1.82(-5)		
1.00	2.92(-4)	0.76	9.10(-6)		
0.90	1.50(-4)	0.71	4.48(-6)		
0.80	6.38(-5)				
0.72	2.62(-5)				
0.65	9.42(-6)				

TABLE II

Source	Range (%)		
	W	Au	U
1) Contribution from internal conversion to the x-ray yields.	0.5 - 4	-	-
2) Contribution from the natural radioactivity of the target to the x-ray yields.	-	-	< 4
3) K_{α}/K_{β} branching ratio.	< 1	< 1	< 1
4) Counting statistics and background subtraction.	0.5 - 3	1-4	1.5-4
5) Backscattered particle yields.	-	< 1	-
6) Total collected charge.	< 1	< 1	1-3
7) Uncertainty in x-ray yield due to uncertainty in incident energy	2 - 5	2 - 3	2-3
8) x-ray detector efficiency.	5	5	5.5
9) Particle detector solid angle.	-	5	-
10) Artificial differential cross section due to uncertainty in angle.	-	2.5	-
11) Uncertainty in the slope $dy_{\alpha}/d\theta$	< 7	< 3	< 12
Total absolute uncertainty.	< 11	< 10	< 15

CAPTIONS TO FIGURES

Figure 1 - X-ray spectra of W resulting from proton bombardment. The upper spectrum was obtained at 2.75 MeV proton energy and the other with the lowest incident energy beam (650 keV) we have employed.

Figure 2 - The fittings of the x-ray yield curves by functions of the type $aE^2(1+bE)\exp(-BE^{-3/2})$. The four adjustable parameters are given in the insert.

Figure 3 - K-shell ionisation cross sections (in barns) versus energy (in MeV). See the text for an explanation of the solid curves. Symbols key: solid circles, this work; W-squares, Gociowski et al 1983; Au and U - open circles, Mamiya et al 1977 and triangles, Anholt 1978a.

Figure 4 - The abscissa is the Coulomb deflection factor. The points are our experimental results divided by σ_{PSSR} . The curves correspond to different calculated factors. Kochach's and Montenegro and the Pinho's factors were calculated for protons on gold.

Figure 5 - The same as figure 4 taking into account the inelastic aspect of the collision in σ_{PSSR} and in the dq_0 variable. The variable x is the modified σ_{dq_0} following the prescription of Braad and Lapicki (1981). Symbols and curves are the same as in figure 4.

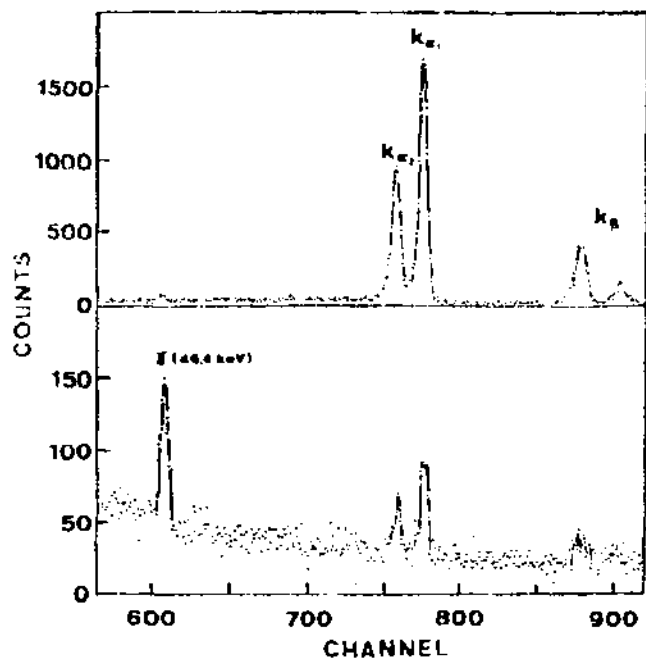


Figure 1

Figure 1

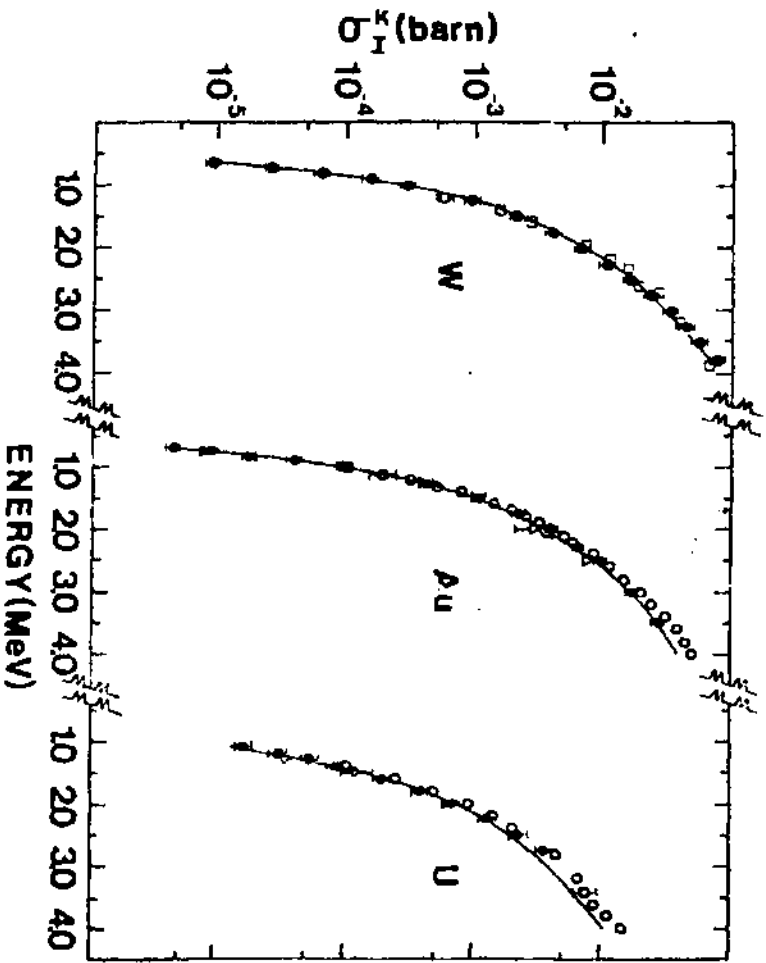
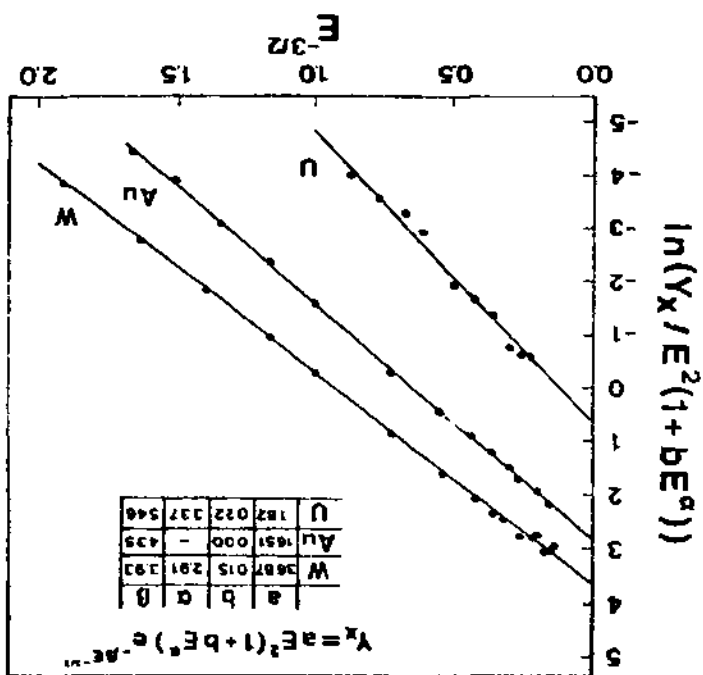


Figure 2



COULOMB FACTOR

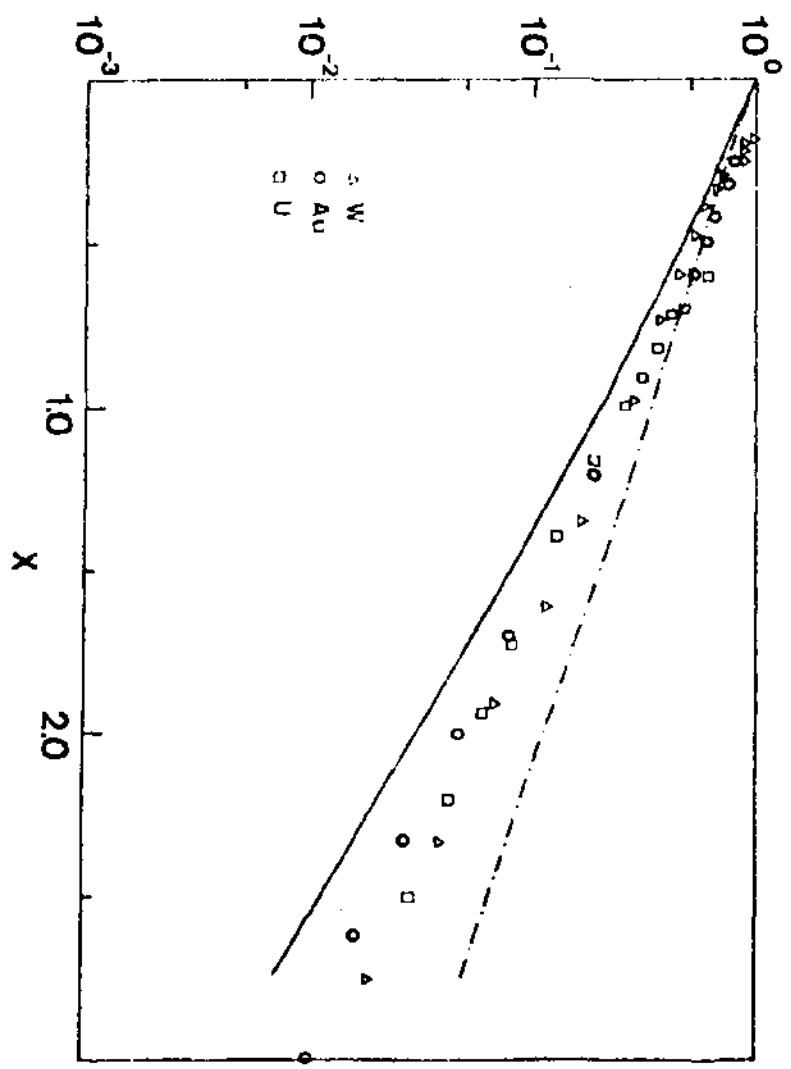


Figure 4

COULOMB FACTOR

